energies

MDPI

Article

Experimenting with a Battery-Based Mitigation Technique for Coping with Predictable Partial Shading

Rosario Carbone [1,*] and Cosimo Borrello [2]

[1] Department "dell'Informazione, delle Infrastrutture e dell'Energia Sostenibile" (D.I.I.E.S), University "Mediterranea" of Reggio Calabria, 89124 Reggio Calabria, Italy
[2] Department "di Ingegneria Civile, dell'Energia, dell'Ambiente e dei Materiali" (D.I.C.E.A.M.), University "Mediterranea" of Reggio Calabria, 89124 Reggio Calabria, Italy; brrcsm95l30h224e@studenti.unirc.it
* Correspondence: rosario.carbone@unirc.it; Tel.: +39-09-651-693-310

Abstract: In this paper, the authors propose to use batteries to improve the performance of grid-connected photovoltaic plants when their photovoltaic fields are subject to partial shading phenomena. Particular attention is devoted to predictable and repetitive partial shadings, such as those that often appear in urban residential environments. Firstly, battery packs with proper nominal voltage and capacity are connected in parallel to partially shaded photovoltaic submodules. Then, the shaded photovoltaic submodules are properly disconnected and connected to the respective photovoltaic string by using a "battery control unit", which is operated by taking into account characteristics of the specific partial shading phenomenon to cope with. To demonstrate the effectiveness of the proposed technique, an experimental study is performed to compare the performances of two identical prototypal grid-connected photovoltaic generators subject to identical artificial and repetitive partial shadings. Only one of the photovoltaic generators is equipped with batteries together with their respective battery control unit, while the second one is simply equipped with conventional bypass diodes. The main advantages of the proposed technique are a greatly improved whole power generation together with the elimination of hotspot phenomena.

Keywords: PV plants; partial shadings; hotspot; bypass diodes; battery storage

check for updates

Citation: Carbone, R.; Borrello, C. Experimenting with a Battery-Based Mitigation Technique for Coping with Predictable Partial Shading. *Energies* **2022**, *15*, 4146. https://doi.org/10.3390/en15114146

Academic Editor: Jong Hoon Kim

Received: 14 May 2022
Accepted: 2 June 2022
Published: 5 June 2022

Publisher's Note: MDPI stays neutral with regard to jurisdictional claims in published maps and institutional affiliations.

Copyright: © 2022 by the authors. Licensee MDPI, Basel, Switzerland. This article is an open access article distributed under the terms and conditions of the Creative Commons Attribution (CC BY) license (https://creativecommons.org/licenses/by/4.0/).

1. Introduction

Partial shadings are one of the most relevant phenomena causing a significant reduction in power generation and damage in photovoltaic (PV) plants [1–5].

In a PV string, the higher the number of PV modules (and PV cells) connected in series, the higher the power generation losses when only a small number of PV cells are shaded. Furthermore, the higher the number of PV cells connected in a series, the more rapidly the voltage of the shaded PV cells reverses, causing power dissipation on the shaded PV cells and leading to an undesired PV cells temperature rise and hotspot phenomena [6–8].

Conventionally, bypass diodes are widely utilized in commercial PV modules to minimize the detrimental effects of partial shading conditions. With some more detail, the series connected PV cells of a PV module are grouped in submodules, and a power diode is connected in antiparallel to each submodule. As an example, PV modules based on the series of sixty connected PV cells are typically grouped in three submodules of twenty PV cells, and they are equipped with three bypass diodes, which are installed in the PV module junction box. In this way, under uniform solar irradiation of the PV module, all the bypass diodes are reverse biased, and they work as an open circuit. In contrast, if only some PV cells of a submodule are shaded and its voltage reverses, its respective bypass diode becomes forward biased, and it conducts the difference between the full current generated by unshaded submodules and the current generated by the shaded submodule. This means that, under partial shadings, thanks to the intervention of the bypass diode, the

unshaded PV cells of an entire PV string can generate their maximum power. Furthermore, the reversed voltage of the shaded submodule (the bypassed submodule) is limited to the direct voltage drop on the bypass diode.

Nevertheless, many studies [9,10] demonstrate that bypass diodes are not the better way to cope with critical partial shading phenomena, and they do not completely avoid hotspot phenomena. Therefore, different alternative solutions have been proposed in the specialized literature [11–21].

One of the most relevant limits of bypass diodes is the additional conduction loss that occurs when they intervene, especially when the maximum power point of the unshaded PV string is in correspondence with a low voltage level [10]; in addition, power dissipation on the bypassed submodule can contribute sensibly to the whole power generation loss of the PV string. Furthermore, some experimental studies [22,23] have shown that PV cells in commercial submodules of widely diffused lengths are susceptible to hot spotting in the presence of conventional bypass diodes because of the spread of solar cell parameters and because of localized dirt, bird droppings, leaves, etc. This effect is accentuated in case only a single cell is partially shaded since it has to dissipate the power of the rest of the cells protected by the same bypass diode. Finally, in [9], it has been evidenced that, in PV modules subject to repeated overheating, there is also the concrete possibility that, in the medium term, bypass diodes degrade or fail.

As mentioned above, to overcome the limits of conventional bypass diodes, different proposals have been presented and discussed in the literature. As a brief overview, in [11–13], submodule-distributed DC–DC power electronic converters are introduced for maximizing power generation in case of partial shadings and also for mitigating hotspot phenomena. In [14,17,20], possible circuit reconfiguration techniques among partially shaded PV modules and submodules are introduced and discussed. In [15,16,19], conventional bypass diodes are proposed to be substituted by different smart bypass circuits. Finally, in [18], the usefulness of introducing small power-distributed battery packs in parallel with shaded submodules has been investigated by means of a first-level experimental study. One of the most relevant advantages of introducing battery storage to cope with partial shadings is that the battery voltage (that is to say, also the shaded submodule voltage) does not reverse and no power dissipation on the shaded submodule occurs. Furthermore, the power generated by the shaded submodule can be saved and injected into the grid together with the maximum power generated by the unshaded PV string, so maximizing the PV string's whole generated power. However, a connection and disconnection procedure of the shaded submodule's battery has to be studied and operated by a proper battery control unit (BCU).

To cope with critical and repetitive partial shading phenomena, we started with the idea introduced in [18], and proposed and experimentally tested the use of a 6V 12 Ah rechargeable lead acid commercial battery at the submodule level. By taking into account characteristics of the specific partial shading phenomenon, firstly, a battery control unit has been designed and built to be operated by a proper connection/disconnection control logic. Then, an experimental comparative analysis of performances is carried out between two identical low-power prototypes of grid-connected PV generators. Each PV generator prototype consists of a 300 Wp 60 PV cells commercial PV module connected in a series by a homemade 60 Wp 18 PV cells submodule to be artificially shaded. For measuring purposes, both homemade submodules have been built so that one can access every single PV cell. In the first PV generator, the homemade submodule is simply equipped with a conventional bypass diode; in contrast, the homemade submodule of the second PV generator has a 6 V 12 Ah battery connected in parallel, together with its respective BCU. Identical partial shadings on both submodules are artificially produced using two fixed opaque sheets. In Section 3, after having better specified the abovementioned prototypes, the results of the experimental analysis are reported and discussed. Finally, the most relevant conclusions about the practical usefulness of our proposal are presented.

2. Description of the Basic Idea

Among the abovementioned techniques proposed in the literature for overcoming limits of conventional bypass diodes in case of critical partial shadings, only in [18] has it been proposed to connect batteries in parallel with partially shaded photovoltaic submodules without any additional circuitry and controlled switches. For similar purposes, in [23], it has been proposed to introduce batteries within the circuitry of DC/DC power electronic converters to mitigate their power conduction losses and to avoid the need for a complex, central maximum-power point-tracking algorithm to be implemented by the central inverter, otherwise needed as proved in [24].

On the other hand, in [25], it has been already demonstrated that batteries, if installed in a distributed manner, can operate as a first-level distributed "passive" MPPT and can improve the energy production of conventional grid-connected PV plants, especially in the presence of mismatching conditions, so representing a valid alternative to distributed active MPPTs. In fact, a battery pack can be profitably connected in parallel with a photovoltaic submodule if one has care to properly match, as best as possible, its nominal voltage with the open-circuit voltage (under STC) of the submodule. For more details, it can be worthwhile to look at Figure 1. It shows that, in parallel with the PV generator and the network, a battery properly designed in its nominal voltage value can naturally catch and maintain a PG working point very close to the maximum power point MPP for any PG solar irradiation level and any value of the grid equivalent resistance.

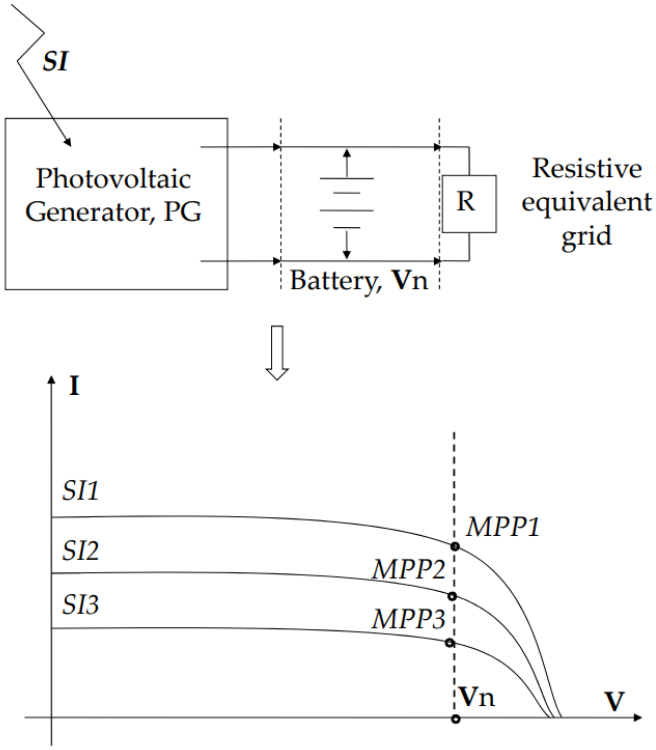

Figure 1. Working point variations of a grid-connected PV generator for different solar irradiance (*SI*) levels in the presence of a battery [25].

Nevertheless, it is expected that batteries used as passive MPPTs have lower performances if compared with active MPPTs, mainly because of the variations in the PV generator working temperature. This is especially true with respect to innovative active MPPT techniques that combine fuzzy logic with fractional PID controllers [26–28]. Furthermore, to make effective battery-based passive MPPTs, batteries' state of charge (SoC) should be continuously monitored and controlled.

Starting from the abovementioned battery properties and studies, in this paper, a proper battery control unit (BCU) is introduced to maximize the benefits of the battery

presence in case of predictable and repetitive partial shadings on a PV field. Firstly, the BCU has the important task of controlling the battery SoC. This can be obtained by connecting or disconnecting the submodule equipped with the battery from the remaining series-connected PV modules of the same PV string when the battery voltage rises above or falls below proper pre-established limits. Furthermore, the BCU also has to make possible the recovery of the power that the partially shaded submodule can generate. This additional task can be obtained by injecting the stored power within the grid, together with the power generated by the unshaded PV modules, during the time intervals in which the generation capacity of the unshaded PV modules is at the maximum. In practice, once designed, the simple circuitry of the BCU is also needed to determine its optimal operating procedure by taking into account the characteristics of the specific, predictable partial shading to cope with. More details about this important task are specified in the next section dedicated to our experimental tests.

As in the previous papers [19,23,25], in this work, batteries are proposed to be utilized in a distributed manner by connecting them at the submodule level of a PV string, but only at the terminals (available within their respective junction box) of the shaded submodules. Figure 2 should give a better understanding of the proposed plant architecture.

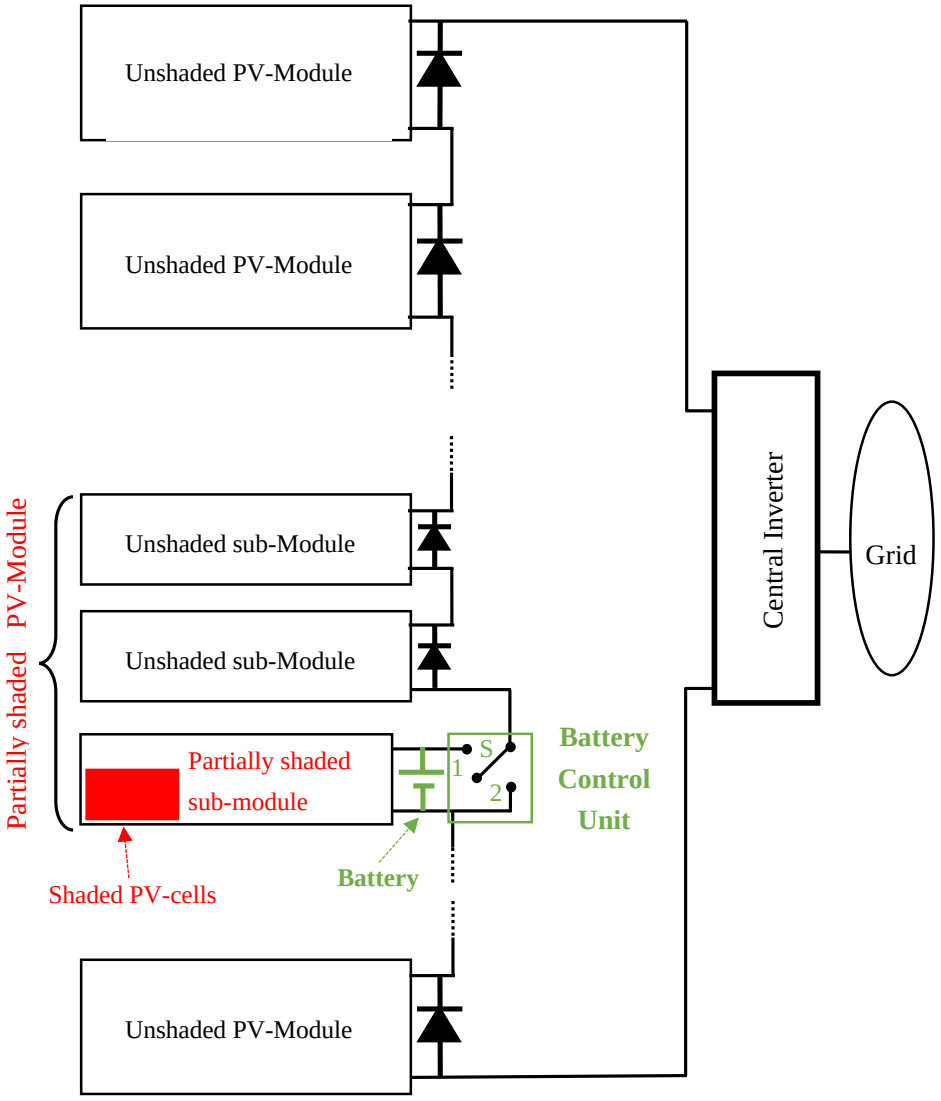

Figure 2. Architecture of the proposed PV plant in the presence of a partially shaded submodule.

In practice, during a whole day, the BCU drives the charge of the battery during the time intervals in which the partial shading in the submodule is low by closing the switch (S) in position 2. During these time intervals, the partially shaded submodule is bypassed, and the remaining series-connected unshaded submodules (and PV modules) of the whole PV string can generate their maximum power, which is injected into the grid by the central inverter. In contrast, the BCU drives the discharge of the battery by closing the switch in position 1. This is performed when the battery is charged and the partial shading on the submodule is strong; in this situation, the battery presence is able to guarantee the shaded submodule is generating the same current as the unshaded series-connected submodules (and PV modules), avoiding any limitation to the potential generation. This means that the whole PV string is now generating the maximum power of the unshaded submodules and PV modules plus the power generated during the day by the partially shaded submodule (except for the charging/discharging power losses of the battery). To avoid both overcharging and too much discharging of the battery, a voltage control system can be used for driving the switch in position 1 during the charging time intervals and for driving the switch in position 2 also during the discharging time intervals.

In addition to the abovementioned advantages in terms of maximization of the daily power generation of the PV string, the proposed architecture also guarantees that the voltage at the terminal of the partially shaded submodule does not reverse, even under severe partial shadings. On the contrary, the voltage at the terminals of the partially shaded submodule always coincides with (about) the positive nominal voltage of the battery. Therefore, the voltage at the terminals of the shaded PV cells within the partially shaded submodule does not reverse, even in the case the shading involves a small number of PV cells [19]. This means that no power dissipation and high temperature and hotspot phenomena involve the PV cells of the partially shaded submodule.

3. Experimental Tests, Results, and Discussions

This section summarizes the results of a campaign of measurements on a small power grid-connected PV generator prototype based on two identical PV strings (each of about 300 Wp) connected in parallel to the distribution grid through two commercial microinverters equipped with a reliable Perturb&Observe MPPT. Measurements involve outdoor different solar irradiation conditions. Repetitive and predictable partial shadings are artificially produced only on a small number of PV cells (on board the aforementioned homemade submodules) in order to give evidence of: (i) their potentially detrimental effects, (ii) limits of conventional bypass diodes, and (iii) the effectiveness of the proposed battery-based mitigation technique.

In the next subsections, firstly, the PV generators under study are better specified by clarifying the characteristics of their fundamental components together with the control logic of the BCU, which is mounted and operated only on one of the homemade submodules. Then, the measurement results of the most significant experiments are reported, compared, and discussed.

3.1. Description of the Prototypal PV Generators and the Battery Control Unit (BCU)

3.1.1. The PV Generators

The tested PV plant consists of two low-power PV generators connected in parallel with the public distribution grid through two microinverters.

Each PV generator consists of a commercial photovoltaic panel connected in series with a homemade submodule specifically built for this experimental study.

Concerning the commercial modules, they are two FuturaSun "FU 300 M", consisting of 60 monocrystalline PV cells for maximum nominal power under STC of about 300 Wp. Instead, the two homemade submodules have been self-built on the basis of 18 polycrystalline cells, each with a maximum power of about 4 Wp. Because the polycrystalline PV cells available for building the homemade submodules have lower power (and lower short-circuit current), with respect to the monocrystalline PV cells of the commercial PV

modules, some mismatching (disturbing) effects could affect our experimental tests. Therefore, the commercial PV modules have always been fully covered by a properly selected semitransparent darkening veil for equalizing their short-circuit current with that of the polycrystalline PV cells. Once this has been achieved, the maximum power of the two commercial PV modules has been reduced to about 250 Wp.

Referring to the study presented in [25], we decided to build the two submodules on the basis of 18 cells to guarantee, as best as possible, the optimal matching between the value of their maximum power voltage (under STC) with the nominal voltage of the commercial battery we have used for our experiments (lead acid, 6 V 12 Ah battery).

Please note that, for purposes of complete measurements, the two submodules have been built by making accessible (through external connectors) each individual PV cell. This feature has allowed us to fully monitor both the submodules together with their shaded and unshaded PV cells.

The microinverters used for connecting the two PV generators to the distribution grid are two "M250-72-2LN-S2" by Enphase Energy Inc., Fremont, CA, USA; they are equipped with a reliable Perturb & Observe MPPT [29]. They are also fully monitored by the communication gateway "Envoy-S" by Enphase Energy Inc. [30]. The generation data of the two microinverters are finally stored and available online thanks to the monitoring software "Enlighten" by Enphase Inc.

Some descriptive pictures of the prototypal generator are included in Figure 3.

Figure 3. Some pictures describing the prototypal PV generator together with the BCU.

3.1.2. The Battery Control Unit (BCU)

As proposed in Section 2, a battery control unit (BCU) is necessary for charging and discharging the battery connected in parallel with the shaded submodule. In this way, the power generated by the partially shaded submodule can be first stored and then injected into the distribution grid through the series-connected unshaded PV module and its respective microinverter. In addition, this procedure also makes possible the control of the battery's state of charge (SoC) to avoid overcharging and extensive discharges.

For obtaining the abovementioned tasks, together with some additional measuring purposes, we have built the BCU by the following list of components:

- An "Arduino Mega" board, mounting an "ATmega 2560" microcontroller, programmed to handle all the BCU control logic;
- A self-designed extensible board (connected to the Arduino board) containing three resistive dividers (for voltage measurements) and three ACS712 ICs by "Allegro" MicroSystems Inc. (Manchester, NH, USA) (for current measurements);
- Opto-isolated relays, to allow variations in circuit connections, as discussed in Section 2;
- A Wi-Fi module ESP8266 by "Espressif Systems", for Internet connection and remote monitoring of the acquired data, saved on a dedicated database;
- A plastic cover, equipped with an LCD and some manual switches for security purposes.

Within the same protective box, we have also installed the connectors, the fuses necessary for realizing all the wired connections, and the 6 V 12 Ah lead acid battery to be connected in parallel with the partially shaded homemade submodule.

Some more detail is reported in the specific pictures included in Figures 3 and 4.

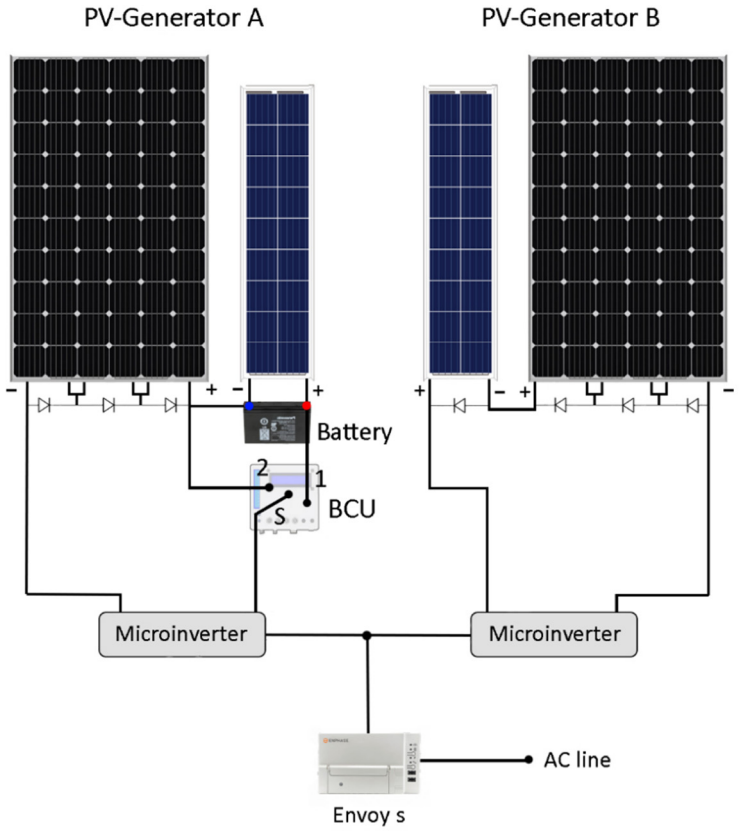

Figure 4. Schematic of the prototypal PV generator equipped with the Battery and the BCU.

About the artificial partial shading to cope with, firstly, please note (Figure 3) that all the PV modules and the homemade submodules are south facing. Then, two opaque plywood sheets are mounted only on the two homemade submodules so that, for each

submodule, only three consecutive PV cells are partially shaded. Because of the mounting characteristics of the PV modules and of the fixed opaque sheets, the partial shading is expected to be repetitive and predictable. In particular, during a single day, the partial shading level of those PV cells is expected to be: (i) low during the morning hours, (ii) very high during the central hours, and (iii) low during the evening hours. Some further details are provided in the following Section 3.2.2.

3.2. Experimental Tests Performed without Introducing the Battery

The two low-power PV generator prototypes (A and B) specified in the previous section have been utilized in making the first group of experiments under different outdoor operating conditions, specifically conceived for testing the advantages and limits of the using the conventional bypass diodes for coping with critical partial shadings. These experiments are grouped in three different case studies and are separately specified and discussed in the following Sections 3.2.1–3.2.3

3.2.1. Results during Cloudless Days and with No Artificial Shadings on the PV Generators

Firstly, the two PV generators, A and B, have been exposed to the sunlight without any shading obstacle or any additional component to demonstrate their almost identical daily energy generation capability. Figure 5 shows the daily power generation curves, Pg_A and Pg_B, of the two PV generators on a July 2021 cloudless day, together with their daily generated energies, Eg_A and Eg_B. Both PV generators have produced almost the same daily energy of about 1.2 kWh.

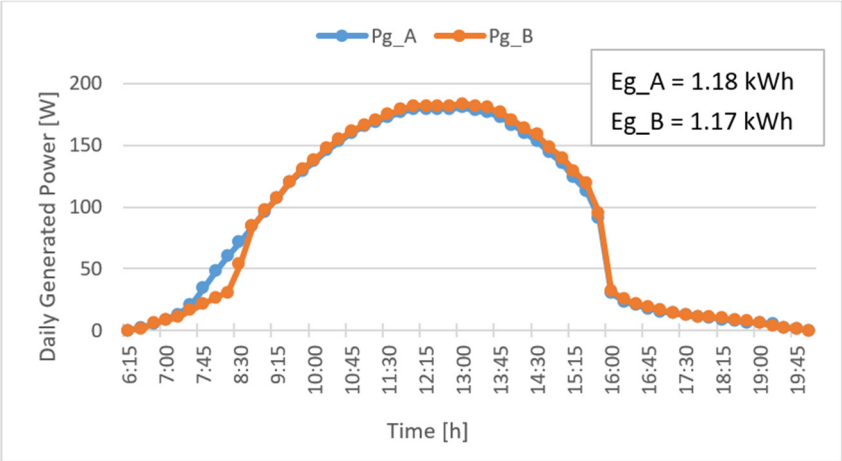

Figure 5. Daily power generation curves, Pg_A and Pg_B, of the two PV generators A and B, on a July 2021 cloudless day, together with corresponding daily generated energy values, Eg_A and Eg_B.

3.2.2. Results during Cloudless Days and with Artificial Shadings Produced Only on the Homemade Submodule of the PV Generator B

The second set of experiments has been dedicated to searching for a critical partial shading opaque obstacle to be mounted only on a small number of consecutive PV cells of the homemade submodule of the PV generator B. With more detail, many opaque shading plywood sheets with different widths have been tested for shading only three consecutive PV cells of the same column of the aforementioned submodule; they have also been mounted at different heights.

In this way, after many attempts, we have found the width of the shading plywood sheet and its mounting height for which the bypass diode of the submodule B does not intervene or intervenes uncertainly. This gave us the possibility to register the maximum loss of the daily energy generation of the shaded PV generator with respect to the unshaded one, together with some other important phenomena. This critical shading plywood sheet

and mounting have been tested for a number of days, and, actually, during this period, the bypass diode intervened randomly.

Figure 6 shows the daily power generation curves, Pg_A and Pg_B, of both PV generators A (with no shading) and B (with shading) together with the corresponding daily generated energies, Eg_A and Eg_B, and the percentage energy loss factor, Loss%, of the PV generator B with respect to the PV generator A. The experiment refers to a July 2021 cloudless day when the bypass diode of the submodule B did not intervene.

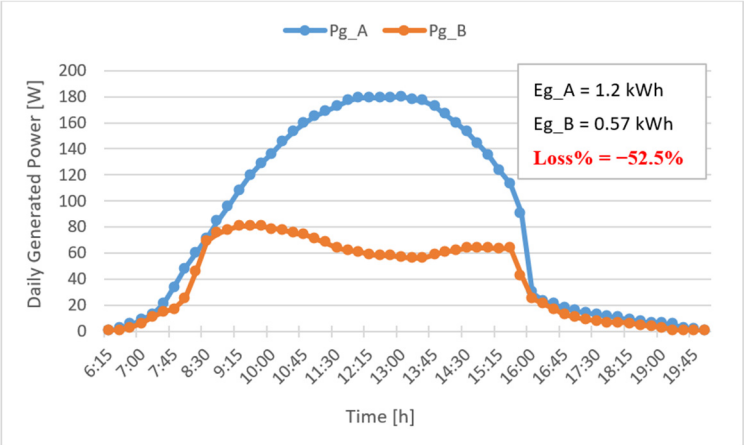

Figure 6. Daily Power generation curves, Pg_A and Pg_B, of the two prototypal PV generators A and B on a July 2021 cloudless day, together with corresponding daily generated energy values, Eg_A and Eg_B, and the percentage energy loss factor, Loss%. In this experiment, an opaque shading plywood sheet was mounted only on three PV cells of the homemade submodule of the PV generator B, and the corresponding bypass diode did not intervene.

Figure 7 shows the daily power generation curves of both PV generators A (with no shading) and B (with shading) during a cloudless day when the bypass diode intervened late.

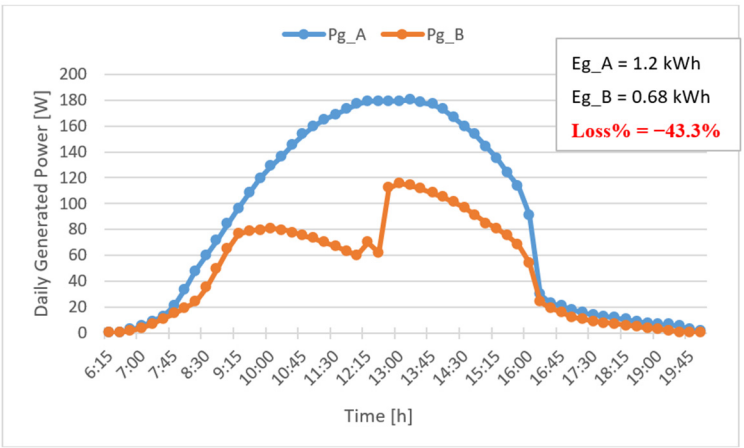

Figure 7. Daily power generation curves, Pg_A and Pg_B, of the two prototypal PV generators A and B on a July 2021 cloudless day, together with corresponding daily generated energy values, Eg_A and Eg_B, and the percentage of energy loss factor, Loss%. In this experiment, a shading plywood sheet was mounted only on three PV cells of the homemade submodule of the PV generator B, and the corresponding bypass diode intervened late, at about 12:30.

Figure 8 shows the daily power generation curves of both PV generators A (with no shading) and B (with shading) during a cloudless day when the bypass diode intervened early, but it left the conduction mode at about 13:00.

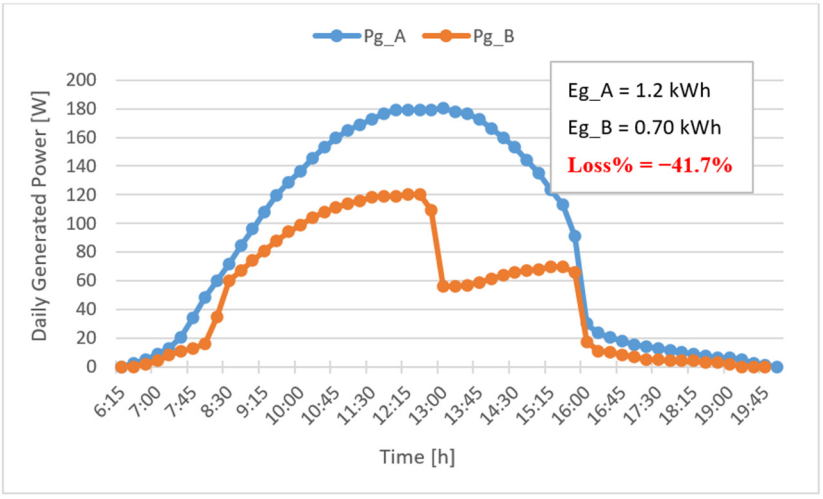

Figure 8. Daily power generation curves, Pg_A and Pg_B, of the two prototypal PV generators A and B on a July 2021 cloudless day, together with corresponding daily generated energy values, Eg_A and Eg_B, and the percentage energy loss factor, Loss%. In this experiment, a shading plywood sheet was mounted only on three PV cells of the homemade submodule of the PV generator B, and the corresponding bypass diode intervened early but left the conduction mode at about 13:00.

Figure 9 shows the daily power generation curves of both the PV generators A (with no shading) and B (with shading) during a cloudless day when the bypass diode intervened early, and it remained in the conduction mode until the evening.

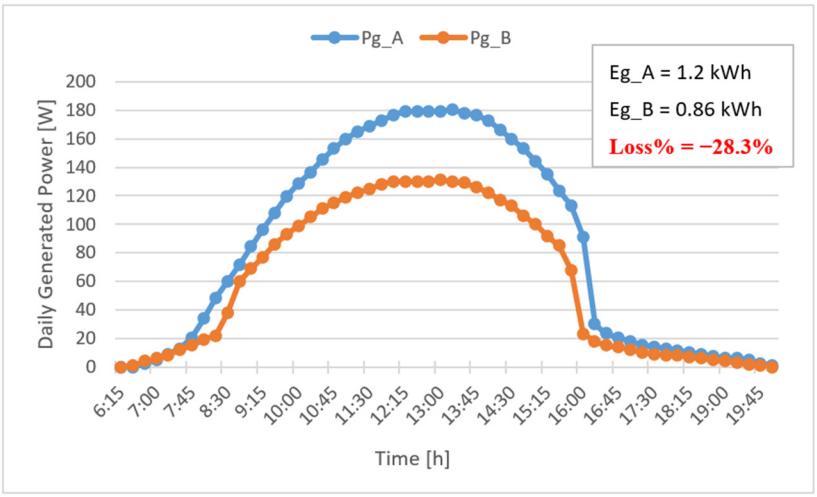

Figure 9. Daily power generation curves, Pg_A and Pg_B, of the two prototypal PV generators A and B on a July 2021 cloudless day, together with corresponding daily generated energy values, Eg_A and Eg_B, and the percentage energy loss factor, Loss%. In this experiment, a shading plywood sheet was mounted only on three PV cells of the homemade submodule of the PV generator B, and the corresponding bypass diode intervened early and remained in the conduction mode until the evening.

Figure 10 shows the daily curves of (i) the current of the whole PV generator B, I_PV_Gen_B, (ii) the current of the three shaded cells on board the submodule of the PV generator B, I_Shaded_Cells, and (iii) the voltage at the terminal of the aforementioned three shaded cells, V_Shaded_cells, when the bypass diode of the submodule of the PV generator B intervened for a long time.

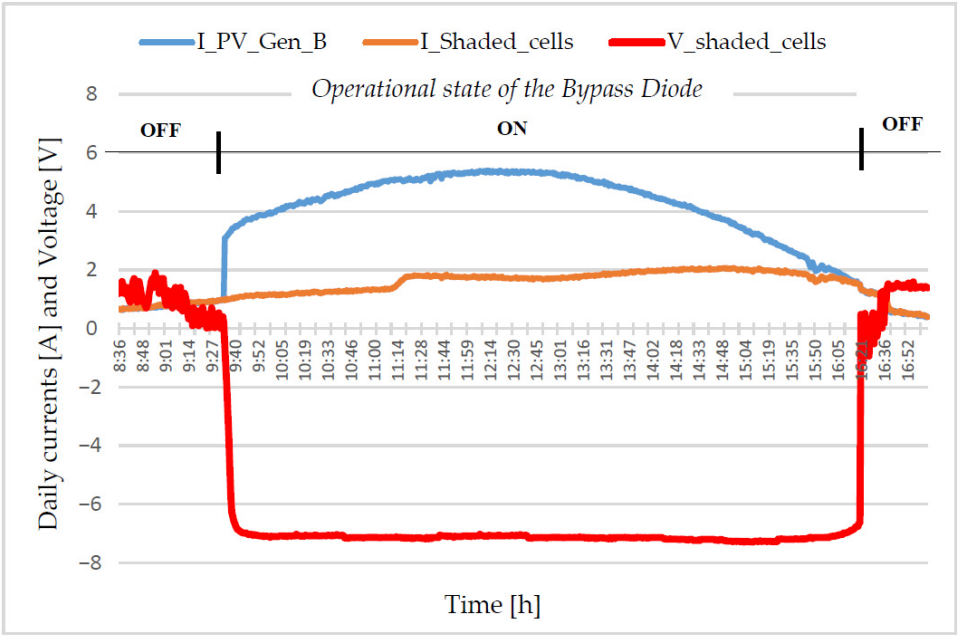

Figure 10. Daily curves of (i) the current of the PV generator B (I_PV_Gen_B), (ii) the current (I_Shaded_cells), and (iii) the voltage (V_Shaded_cells) of the three shaded cells of the submodule of the PV generator B, when the bypass diode intervened for a long time.

3.2.3. Discussion and Additional Short-Time Experiment

Figures 6–10 clearly show that for certain critical partial shadings, conventional bypass diodes do not intervene or intervene randomly, and they are not able to avoid a very significant loss of energy generation (as far as more than 50%).

Figure 6 shows that when the bypass diode does not intervene, the partial shading of our case study causes a significant reduction in the generation power of the PV generator B, especially starting from about 9:30 in the morning to about 15:30 in the afternoon, with a peak of the power losses at about the midday.

Figure 9 shows that when the bypass diode intervenes, generation losses are greatly reduced; they remain noticeable, also depending criticality on the partial shading.

Furthermore, from Figure 10, some additional and very interesting phenomena can be outlined. Firstly, it is easy to remark that when the bypass diode is not in the conduction mode (OFF state), the currents I_PV_Gen_B and I_Shaded_cells coincide. In contrast, during the extended time when the bypass diode is in the conduction mode (ON state), the current I_Shaded_cells is lower than the current I_PV_Gen_B because a new current (the difference) is now flowing in the bypass diode. The exact value of the current I_Shaded_cells depends on the severity of the shading; in our experiment, it resulted in being about 2 Amps for a long time, while the current of the whole PV generator B reached the major value of more than 5 Amps.

At the same time, when the bypass diode is in the conduction mode, the voltage at the terminal of the shaded cells, V_shaded_cells, reverses, reaching and maintaining for a long-time a value of about −7 Volts.

This means that, during the long-time conduction mode of the bypass diode, the three shaded cells are in the reverse-bias condition and, instead of generating, they are forced to dissipate a significant amount of power; in our case, about 14 W.

As already recalled in Section 1, the aforementioned phenomenon is well known, and it has also been theoretically studied and experimentally demonstrated in detail [18,21]. In particular, in such papers, it has been shown that, depending on the construction features (or defects) of a certain PV cell and also on the number of series-connected PV cells protected by a bypass diode, the exposure to a critical reverse bias (i.e., caused by partial shading)

may lead to critical localized over-temperatures and, sometimes, also to the catastrophic failure of a single PV cell.

For these reasons, to avoid possible permanent damage to our homemade PV modules during long time experiments, we decided to give experimental evidence of this phenomenon by using a string or a series of (the homemade submodule) eighteen connected PV cells protected by a bypass diode and by shading a group (series) of three PV cells (instead of a single PV cell). In this way, the revealed/measured 14 W power, dissipated during the reverse bias time, has affected a group of three consecutive connected shaded PV cells, and no dangerous increased temperatures have been registered on them.

However, once this phenomenon was experimentally evidenced together with his danger level, we decided to perform an additional short-time experiment by shading in a very similar way only a single PV cell during the central hours of the next cloudless July day. During this additional experiment, we have constantly monitored the conduction mode of the bypass diode together with the reverse voltage, the current, and the temperature of the shaded PV cell; this last was measured by an infrared IR Fluke 61 thermometer. As in the previous experiment, the bypass diode suddenly entered and remained in the conduction mode, and the reverse voltage and the current of the PV cell have respectively reached the values of about −7 V and 2 A. In a small area close to a corner of the shaded PV cell, the temperature rapidly increased compared with temperatures of different areas and different PV cells; furthermore, after some minutes, it reached the dangerous value of 105 °C, just long enough for us to decide to stop the experiment to avoid damage to the homemade module; the (not tempered) glass cover was noticeably cracked while the polystyrene back sheet was also noticeable fused. The photos in Figure 11 reveal some more illustrative details.

Figure 11. Some damage on the homemade submodule, when only a single PV cell has been partially shaded, and the bypass diode of the submodule intervened.

In our opinion, these experimental results are enough to confirm that conventional bypass diodes are not able to cope effectively with critical partial shadings.

Therefore, the next section refers to a new group of experiments performed by mounting and operating our proposed battery-based mitigation technique, already described and specified in the previous Sections 2 and 3.1.2.

3.3. Experimental Tests Performed by Introducing and Operating the Proposed Battery Control Unit (BCU)

The two low-power PV generator prototypes (A and B) are now utilized for making the second group of experiments under different outdoor operating conditions, specifically conceived for testing the advantages of introducing and operating the proposed BCU specified in the Sections 2 and 3.1.2, for coping with the same critical partial shadings tested in Section 3.2.

With this aim, two identical opaque plywood sheets are now mounted on both PV generators A and B for shading only three consecutive PV cells of their respective homemade submodules.

The proposed battery control unit described in Section 3.1.2 is introduced and operated only on the PV generator A.

To find the optimal control logic for operating the BCU, firstly, we have analyzed the specific characteristics of the power generation losses caused by the artificial partial shading under study, as already evidenced in Figure 5 and outlined in Section 3.2.3. From this analysis, we decided to maintain the partially shaded homemade submodule and its parallel mounted 6 V battery disconnected from the unshaded commercial PV module (switch S in position 2, in Figure 2) from the sunrise until about 11:00 and again from about 15:00 until the evening. This is because, in these time intervals, the submodule suffers from a low level of partial shading, and it results in being able to transfer its generated energy to the battery. To avoid overcharging of the battery, in these time intervals, an over-voltage control function is also activated by the BCU, already referred to in Section 2. From about 11:00 to 15:00, the shaded submodule (and its parallel mounted 6 V battery) has been connected to the grid (switch S in position 1, in Figure 2) through the commercial PV module and the respective microinverter. In this time interval, the submodule suffers from a high level of shading, and it is not able to generate a significant amount of power. In contrast, the already charged battery is able to generate the same current as the unshaded commercial PV module and inject into the grid the power before it is received from the submodule, together with the maximum power generated by the unshaded commercial PV module. To avoid extensive discharge of the battery, in this time interval, an undervoltage control function is also activated by the BCU, as already referred to in Section 2.

As in previous experiments, a conventional bypass diode is mounted on the homemade submodule of the PV generator B.

Results

Figure 12 reports the daily power generation curves, Pg_A and Pg_B, during an August 2021 cloudless day, together with the corresponding daily generated energy values, Eg_A and Eg_B, and the consequent percentage major generation factor, MGF%, of the PV generator A with respect to the PV generator B. In this experiment, the bypass-diode of the submodule of the PV generator B did not intervene.

Figure 13 reports the experimental results during an August 2021 cloudless day when the bypass-diode of the submodule of the PV generator B late intervened.

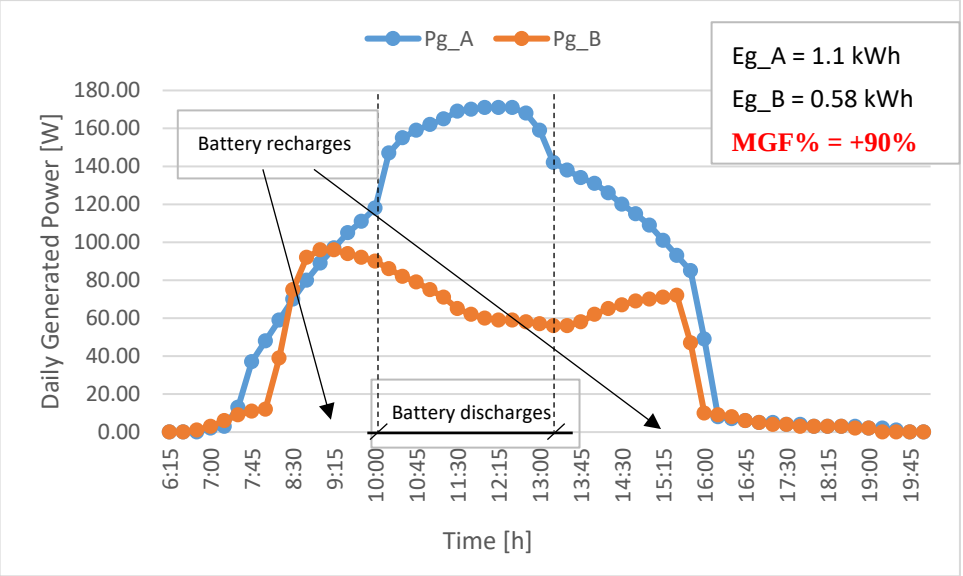

Figure 12. Daily power generation curves, Pg_A and Pg_B, of the two prototypal PV generators A and B on an August 2021 cloudless day, together with the corresponding daily generated energy values, Eg_A and Eg_B, and the percentage major generation factor, MGF%. In this experiment, two identical shading plywood sheets were mounted on three PV cells of both homemade submodules of the PV generator A and B. On the submodule of the PV generator A, the battery control unit was activated while the bypass-diode of the submodule of the PV generator B did not intervene.

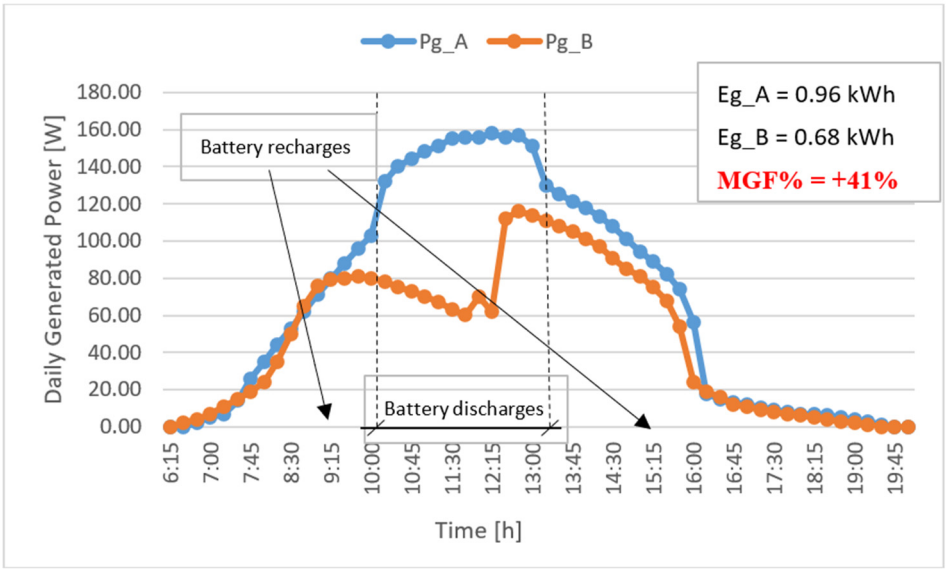

Figure 13. Daily Power generation curves, Pg_A and Pg_B, of the two prototypal PV generators A and B on an August 2021 cloudless day, together with the corresponding daily generated energy values, Eg_A and Eg_B, and the percentage major generation factor, MGF%. In this experiment, two identical shading plywood sheets have been mounted on three PV cells of both the homemade submodules of the PV generator A and B. On the submodule of the PV generator A the battery control unit was activated while the bypass diode of the submodule of the PV generator B intervened late, at about 12:30.

Figure 14 reports the experimental results during an August 2021 cloudless day when the bypass-diode of the submodule of the PV generator B intervened early, but it left the conduction mode at about 13:00.

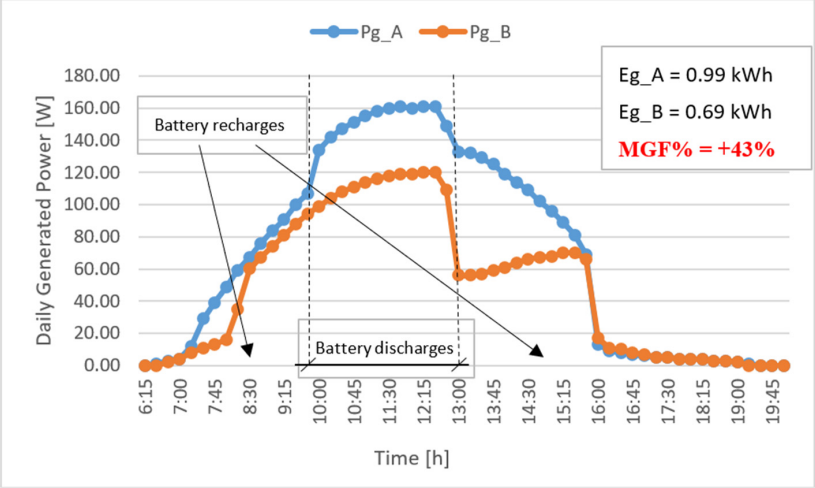

Figure 14. Daily power generation curves, Pg_A and Pg_B, of the two prototypal PV generators A and B on an August 2021 cloudless day, together with the corresponding daily generated energy values, Eg_A and Eg_B, and the percentage major generation factor, MGF%. In this experiment, two identical shading plywood sheets were mounted on three PV cells of both homemade submodules of the PV generator A and B. On the submodule of the PV generator A, the battery control unit was activated while the bypass diode of the submodule of the PV generator B intervened early, but it left the conduction mode at about 13:00.

Figure 15 reports the experimental results during an August 2021 cloudless day when the bypass diode of the submodule of the PV generator B intervened early, and it remained in the conduction mode until the evening.

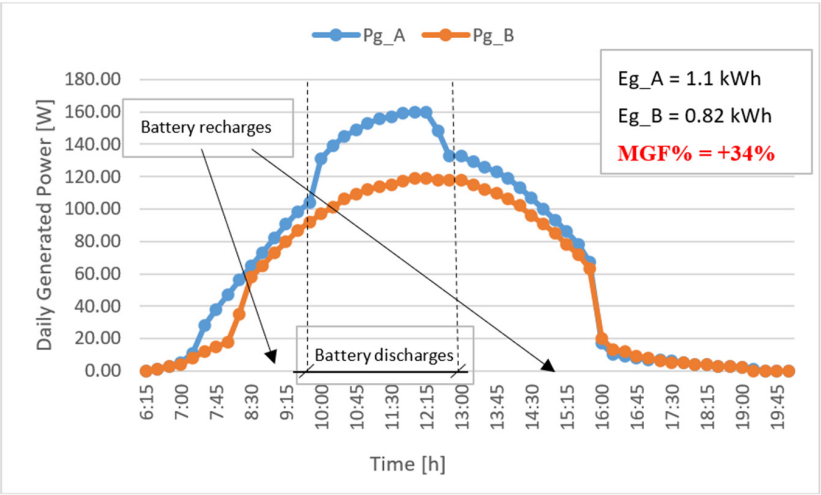

Figure 15. Daily Power generation curves, Pg_A and Pg_B, of the two prototypal PV generators A and B on an August 2021 cloudless day, together with the corresponding daily generated energy values, Eg_A and Eg_B, and the percentage major generation factor, MGF%. In this experiment, two identical shading plywood sheets were mounted on three PV cells of both homemade submodules of the PV generator A and B. On the submodule of the PV generator A, the battery control unit was activated while the bypass diode of the submodule of the PV generator B intervened early, and it remained in the conduction mode until the evening.

In the next experiment, performed on an August 2021 cloudless day, the three PV cells of the homemade submodules of the PV generator A are again shaded with the same opaque plywood sheet and the battery control unit is activated while the PV generator B is now completely unshaded.

Figure 16 reports the daily power generation curves, Pg_A and Pg_B, together with the corresponding daily generated energy values, Eg_A and Eg_B, and the percentage loss factor, Loss%, of the PV generator A compared with the unshaded PV generator B. Additionaly, for this last case study, Figure 17 reports the battery's daily charge and discharge current curves together with its actual voltage curve and the values of its state of charge (SoC). The battery SoC values are estimated offline [31,32] only in correspondence to most relevant time occurrences by accounting for both the battery voltage and the charge and discharge current curves together with other nominal characteristics of the battery [33].

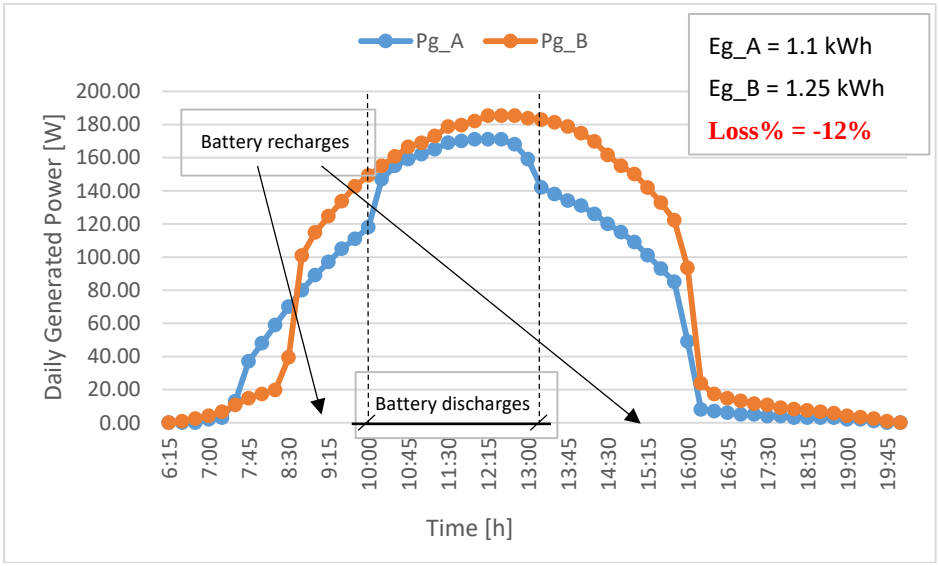

Figure 16. Daily power generation curves, Pg_A and Pg_B, of the two prototypal PV generators A and B, on an August 2021 cloudless day, together with the corresponding daily generated energy values, Eg_A and Eg_B, and the percentage loss factor, Loss%, of the PV generator A compared with the PV generator B. In this experiment, the three PV cells of the homemade submodules of the PV generator A are again shaded, and the battery control unit is activated, while the PV generator B is now completely unshaded.

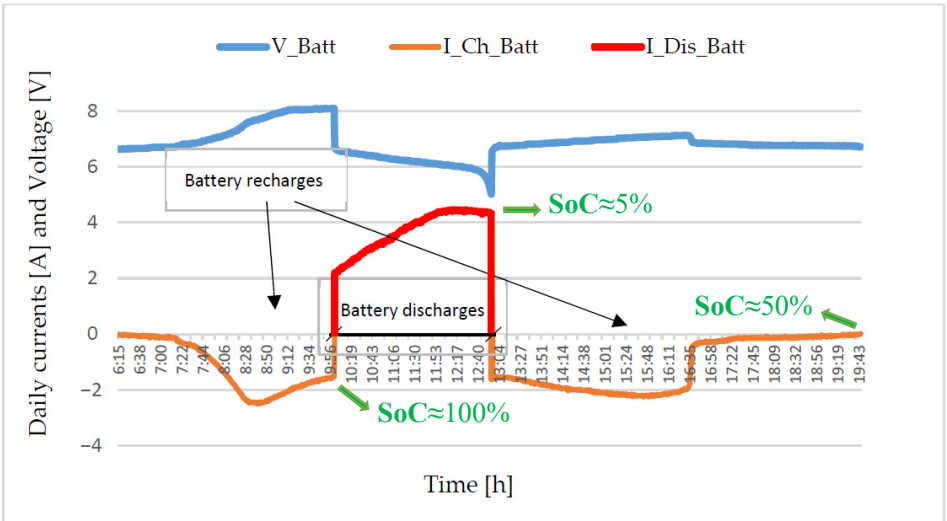

Figure 17. Daily curves of (i) the charging current of the battery (I_Ch_Batt), (ii) the discharging current of the battery (I_Dis_Batt), and (iii) the voltage of the battery (V_Batt) during the experiment referred to in Figure 16. The values of the state of charge (SoC) of the battery are also reported, as estimated offline in correspondence to most relevant time occurrences.

A final and concise discussion of the results of the experimental tests is summarized in the concluding section.

4. Conclusions

In the paper, a battery pack and a battery control unit (BCU) have been experimented with at the submodule level as an alternative to conventional bypass diodes to improve the performance of the grid-connected photovoltaic plants when their photovoltaic fields are subject to predictable and repetitive partial shading phenomena.

Figures 12–15 clearly demonstrate that the proposed technique is always more effective than conventional bypass diodes. In fact, for any conduction state of the bypass diode of the shaded submodule, the daily energy generated by the PV generator equipped with the BCU is always significantly higher than the daily energy generated by the PV generator equipped simply with the bypass diode.

Furthermore, the BCU is always able to prevent the voltage reverse at the terminal of the shaded PV cells and, therefore, also any power dissipation and increased temperature on the shaded PV cells.

Figure 16 also reveals that, by introducing and operating the proposed BCU, the energy generation losses caused by the partial shading case study here analyzed can be drastically reduced from more than 50% (in the worst case in which the conventional bypass diode did not intervene) to a little more than 10%.

Finally, far from an experimental academic scenario such as the one we are now discussing, the hardware strictly necessary for the construction of the BCU (a 6 V 12 Ah lead acid battery, a 10 A relay, and all the remaining electronic components of the BCU) can be achieved at a low cost; we can estimate the cost lower than EUR 25. Obviously, the payback time of these additional costs strongly depends on the severity of the partial shading and its ability to cope with the nominal power of the unshaded PV string connected in series with the shaded submodule: the higher the severity of the partial shading and the higher the nominal power of the series of unshaded connected PV modules, the shorter the payback time. In addition, the battery life has an important impact on the payback time. From this last point of view, the results reported in Figure 17 reveal that, for catching the maximum energy generated by the submodule, we have charged and discharged the battery at the maximum of its capability at the expense of the battery lifetime. A higher capacity battery would probably have been more suitable for our experiment case study.

Author Contributions: Conceptualization, R.C.; Data curation, R.C. and C.B.; Formal analysis, R.C.; Methodology, R.C.; Resources, C.B.; Software, C.B.; Supervision, R.C.; Validation, R.C.; Writing—original draft, R.C. All authors have read and agreed to the published version of the manuscript.

Funding: This research received no external funding.

Conflicts of Interest: The authors declare no conflict of interest.

References

1. Alonso-Gracia, M.C.; Ruiz, J.M.; Chenlo, F. Experimental study of mismatch and shading effects in the I–V characteristic of a photovoltaic module. *Sol. Energy Mater. Sol. Cells* **2006**, *90*, 329–340. [CrossRef]
2. Dolara, A.; Lazaroiu, G.C.; Leva, S.; Manzolini, G. Experimental investigation of partial shading scenarios on PV (photovoltaic) modules. *Energy* **2013**, *55*, 466–475. [CrossRef]
3. Torres, J.P.N.; Nashih, S.K.; Fernandes, C.A.F.; Leite, J.C. The effect of shading on photovoltaic solar panels. *Energy Syst.* **2018**, *9*, 195–208. [CrossRef]
4. Trzmiel, G.; Głuchy, D.; Kurz, D. The Impact of Shading on the Exploitation of Photovoltaic Installations. *Renew. Energy* **2020**, *153*, 480–498. [CrossRef]
5. Abdullah, G.; Nishimura, H.; Fujita, T. An Experimental Investigation on Photovoltaic Array Power Output Affected by the Different Partial Shading Conditions. *Energies* **2021**, *14*, 2344. [CrossRef]
6. Daniele Rossi, D.; Omaña, M.; Giaffreda, D.; Metra, C. Modeling and detection of hotspot in shaded photovoltaic cells. *IEEE Trans. Very Large Scale Integr. (VLSI) Syst.* **2014**, *23*, 1031–1039. [CrossRef]
7. Bayrak, F.; Ertürk, G.; Oztop, H.F. Effects of partial shading on energy and exergy efficiencies for photovoltaic panels. *J. Clean. Prod.* **2017**, *164*, 58–69. [CrossRef]

8. Mohammed, H.; Kumar, M.; Gupta, R. Bypass diode effect on temperature distribution in crystalline silicon photovoltaic module under partial shading. *Sol. Energy* **2020**, *208*, 182–194. [CrossRef]
9. Zhang, Z.; Wohlgemuth, J.; Kurtz, S. Thermal Reliability Study of Bypass Diodes in Photovoltaic Modules (Poster). Presented at the 2013 Photovoltaic Module Reliability Workshop, Golden, CO, USA, 26–27 February 2013. Report Number(s) NREL/PO-5200–58225.
10. Teo, J.C.; Rodney Tan, H.G.; Mok, V.H.; Vigna Ramachandaramurthy, K.; Tan, C. Impact of bypass diode forward voltage on maximum power of a photovoltaic system under partial shading conditions. *Energy* **2020**, *191*, 116491. [CrossRef]
11. Olalla, C.; Rodriguez, M.; Clement, D.; Maksimovic, D. Architectures and Control of Submodule Integrated DC-DC Converters for Photovoltaic Applications. *IEEE Trans. Power Electron.* **2012**, *28*, 2980–2997. [CrossRef]
12. Pilawa-Podgurski, R.C.N.; Perreault, D.J. Submodule integrated distributed maximum power point tracking for solar photovoltaic applications. *IEEE Trans. Power Electron.* **2013**, *28*, 2957–2967. [CrossRef]
13. Solorzano, J.; Egido, M.A. Hot-spot mitigation in PV arrays with distributed MPPT (DMPPT). *Sol. Energy* **2014**, *101*, 131–137. [CrossRef]
14. Parlak, K.S. PV array reconfiguration method under partial shading conditions. *Int. J. Electr. Power Energy Syst.* **2014**, *63*, 713–721. [CrossRef]
15. Bauwens, P.; Doutreloigne, J. Reducing partial shading power loss with an integrated Smart Bypass. *Sol. Energy* **2014**, *103*, 134–142. [CrossRef]
16. Daliento, S.; Di Napoli, F.; Guerriero, P.; D'Alessandro, V. A modified bypass circuit for improved hot spot reliability of solar panels subject to partial shading. *Sol. Energy* **2016**, *134*, 211–218. [CrossRef]
17. Ranjan, P.; Sasmita, S.; Sharm, J.R. Power enhancement from partially shaded modules of solar PV arrays through various interconnections among modules. *Energy* **2018**, *144*, 839–850. [CrossRef]
18. Carbone, R.; Maiolo, G.A. Experimenting a Distributed Passive MPPT based on Mini-Battery-Packs to Cope with Short-Term Critical Partial Shadings on PV–Generators. *IIETA Int. J. Model. Meas. Control B* **2018**, *87*, 113–121. [CrossRef]
19. Daliento, S.; Guerriero, P.; Tricoli, P. A bypass circuit for avoiding the hot spot in PV modules. *Sol. Energy* **2019**, *181*, 430–438.
20. Wen, Z.; Chen, J.; Cheng, X.; Niu, H.; Luo, X. A new and simple split series strings approach for adding bypass diodes in shingled cells modules to reduce shading loss. *Sol. Energy* **2019**, *184*, 497–507. [CrossRef]
21. Kim, K.A.; Krein, P.T. Reexamination of Photovoltaic Hot Spotting to Show Inadequacy of the Bypass Diode. *IEEE J. Photovolt.* **2015**, *5*, 1435–1441. [CrossRef]
22. Ko, S.W.; Ju, Y.C.; Hwang, H.M.; So, J.H.; Jung, Y.S.; Song, H.J.; Song, H.E. Electrical and thermal characteristics of photovoltaic modules under partial shading and with a damaged bypass diode. *Energies* **2017**, *128*, 232–243. [CrossRef]
23. Carbone, R. PV plants with distributed MPPT founded on batteries. *Sol. Energy* **2015**, *122*, 910–923. [CrossRef]
24. Vitelli, M. On the necessity of joint adoption of both distributed maximum power point tracking and central maximum power point tracking in PV systems. Progress in photovoltaics. *Res. Appl.* **2014**, *22*, 283–299. [CrossRef]
25. Carbone, R. Grid-connected photovoltaic systems with energy storage. In Proceedings of the IEEE International Conference on Clean Electrical Power, Capri, Italy, 9–11 June 2009; pp. 760–767. [CrossRef]
26. Assam, B.; Messalti, S.; Harrag, A. New improved hybrid MPPT based on backstepping-sliding mode for PV system. *J. Eur. Syst. Autom.* **2019**, *52*, 317–323. [CrossRef]
27. Babes, B.; Albalawi, F.; Hamouda, N.; Kahla, S.; Ghoneim, S.S.M. Fractional-Fuzzy PID Control Approach of Photovoltaic-Wire Feeder System (PV-WFS): Simulation and HIL-Based Experimental Investigation. *IEEE Access* **2021**, *9*, 159933–159954. [CrossRef]
28. Babes, B.; Boutaghane, A.; Hamouda, N. A novel nature-inspired maximum power point tracking (MPPT) controller based on ACO-ANN algorithm for photovoltaic (PV) system fed arc welding machines. *Neural Comput. Appl.* **2011**, *34*, 299–317. [CrossRef]
29. Enphase Energy; Enphase Microinverters Data Sheet. Available online: https://www4.enphase.com/sites/default/files/downloads/support/M250-DS-EN-UK.pdf (accessed on 26 May 2022).
30. Enphase Energy; Envoy-S Metered—Quick Install Guide. Available online: https://enphase.com/download/envoy-s-metered-installation-guide (accessed on 26 May 2022).
31. Coleman, M.; Lee, C.K.; Zhu, C.; Hurley, W.G. State-of-Charge Determination from EMF Voltage Estimation: Using Impedance, Terminal Voltage, and Current for Lead-Acid and Lithium-Ion Batteries. *IEEE Trans. Ind. Electron.* **2007**, *54*, 2550–2557. [CrossRef]
32. Surendar, V.; Mohankumar, V.; Anand, S.; Prasanna Vadana, D. Estimation of State of Charge of a Lead Acid Battery Using Support Vector Regression. *Procedia Technol.* **2015**, *21*, 264–270. [CrossRef]
33. KON.EL.CO. S.p.A; SKB 6V 12Ah battery Data Sheet. Available online: http://konelco.it/media_prodotti/manuali/38621005_datasheet.pdf (accessed on 31 May 2022).